Acta Technica 62 (2017), No. 6B, 667–676 

# Spatial recursive likelihood identification of multivariable bilinear unmanned aerial vehicle for air quality testing

Junjun Liu[1], Jun Zhang[2]

**Abstract.** In order to improve the accuracy of spatial recursive likelihood identification of multivariable bilinear unmanned aerial vehicle, a spatial recursive likelihood identification method of multivariable bilinear unmanned aerial vehicle based on differential evolution algorithm is proposed. Firstly, give the aerodynamic parameter model of multivariable bilinear unmanned aerial vehicle, ignore the elastic movement, take dynamic differential equations of rigid body with six degrees of freedom as main governing equation, and ignore the inertia moment of dynamical system. Secondly, in order to realize the identification of above model, a spatial recursive likelihood identification method based on differential evolution algorithm is proposed to achieve the effective identification on model. Finally, verify the performance superiority of proposed algorithm by the identification comparison simulation of unmanned aerial vehicle model.

**Key words.** Differential evolution, Multivariable, Unmanned aerial vehicle, Spatial identification.

## 1. Introduction

The spatial recursive likelihood identification is firstly proposed for linear system. In the case of strong-nonlinearity, traditional identification algorithm cannot reach the purpose of identification optimization due to the large deviation between output prediction and actual condition caused by the use f linear model, thus it must be predicted and optimized on the base of nonlinear spatial identification model. The

[1]College of Information Engineering, Zhengzhou University of Science and Technology, Zhengzhou, Henan, 450064, China

[2]College of Electrical Engineering, Zhengzhou University of Science and Technology,Zhengzhou, Henan, 450064, China

common nonlinear modeling method at present includes: mechanism model, Volterra model, Hammerstein model and Wiene model. Establishing mechanism model is required to fully understand the controlled object. However in the case of complex process of production process and multiple connected factors, the establishment of mechanism model usually is difficult. A large-scale device test is required for some special models, such as Volterra, Harstein and Wiene, so the identification cost is very high. Comparing with linear MPC, the example of nonlinear MPC applied in Industry is few, and the most major problem is the high cost for nonlinear process modeling and identification. Therefore, it is very important to find a nonlinear model identification method with lower cost.

In the past 20 years, spatial model identification (SMI) has attracted great attention. It is not only thanks to its excellent convergence and convent numerical computation, but also because it is more suitable for estimate, predict and control the algorithm. In previous references, most spatial identification method is provided with the character of open-loop identification. Considering the stable, safe and control-oriented identification problems, researchers have been trying to apply these spatial methods on closed-loop identification. The spatial method is expanded to the estimation of frequency response function and continuous and discrete time models are determined by auxiliary variable in Literature [9]. Two analytical methods for frequency statistic characteristics and spatial convergence are proposed in Literature [10]. As to the linear closed-loop system in which the external input is irrelevant to the noise observed, the cross-correlation function of output and external input signals are equal to the cross-correlation function of output and external input signals through dynamic system. Therefore, the relationship between the sequences of two related functions can be entirely determined, and the unbiased parameter estimation under any noise characteristic can be obtained. Take the sequence of characteristic-correlated function as interface function. The important information carried by it is hidden in the compression-correlated function form in data sequence. It provides basis for parameter identification by extracting the interface function information of the parameter.

Aiming at the model identification of unmanned aerial vehicle, a spatial recursive likelihood identification algorithm of multivariable bilinear unmanned aerial vehicle based on differential evolution algorithm is proposed, thus the unbiased parameters estimation under the condition of closed-loop dynamics with linear invariant system can be obtained. The solution is to achieve the estimation of correlation function by using the translation invariance of dynamic system.

## 2. Aerodynamic parameter model of multivariable bilinear unmanned aerial vehicle

As to the multivariable bilinear unmanned aerial vehicle, ignore the elastic movement, take dynamic differential equations of rigid body with six degrees of freedom as main governing equation, and ignore the inertia moment of dynamical system. Aiming at the aerodynamic identification in the normal flight range of low-speed mini UAV, the aerodynamic mathematical model of lift force, resistance, rolling moment, pitching moment and yawing moment coefficient in main governing equation $C_L$, $C_D$, $C_Q$, $C_l$, $C_m$ and $C_n$ can be expressed as:

$$\begin{cases} C_L = C_{L0} + C_{L\alpha}\Delta\alpha + C_{Lq}\dfrac{q\bar{c}}{2V^*} + C_{LV}\dfrac{V - V_*}{V^*} + C_{L\delta e}\delta_e\,, \\ C_D = C_{D0} + C_{D\alpha}\Delta\alpha + C_{D\alpha^2}\Delta\alpha^2 + C_{DV}\dfrac{V - V_*}{V_*}\,, \\ C_Q = C_{Q0} + C_{Q\beta}\beta + C_{Qp}\dfrac{qb}{2V_*} + C_{Qr}\dfrac{rb}{2V_*} + C_{Q\delta_r}\delta_r + C_{QV}\dfrac{V - V_*}{V_*}\,, \\ C_l = C_{l0} + C_{l\beta}\beta + C_{lp}\dfrac{pb}{2V_*} + C_{lr}\dfrac{rb}{2V_*} + C_{l\delta_a}\delta_a + C_{l\delta_r}\delta_r\,, \\ C_m = C_{m0} + C_{m\alpha}\Delta\alpha + C_{mq}\dfrac{q\bar{c}}{2V_*} + C_{mV}\dfrac{V - V_*}{V_*} + C_{m\delta e}\delta_e\,, \\ C_n = C_{n0} + C_{n\beta}\beta + C_{np}\dfrac{pb}{2V_*} + C_{nr}\dfrac{rb}{2V_*} + C_{n\delta_a}\delta_a + C_{n\delta_r}\delta_r\,. \end{cases} \tag{1}$$

Where, $V_*$ is the trimming airspeed at operating point in above formulas. Comparing with normal linear aerodynamic model, $C_{Q0}, C_{l0}, C_{n0}$ introduced in model mainly consider the real existence of asymmetric external force effect in actual flight, and apparent asymmetry also will be introduced by the measuring error. However considering the essence of aerodynamic modeling, those errors shall be filtered out firstly, and the errors have not been removed also will be reflected in asymmetric terms. $C_{LV}$, $C_{QV}$ and $C_{mV}$ are the aerodynamic derivatives caused by velocity changes. Although the flight speed is at low Mach, the influence of propulsion system on aerodynamic characteristics in actual flight cannot be ignored, thus such derivatives are introduced, the influence of identification speed change on aerodynamic coupling of propulsion system.

The observational equations used in aerodynamic identification are:

$$\begin{cases} V_m = V + v_V, \alpha_m = \alpha + v_a, \beta_m = \beta + v_\beta\,, \\ p_m = p + v_p, q_m = q + v_q, r_m = r + v_r\,, \\ \varphi_m = \varphi + v_\varphi, \theta_m = \theta + v_\theta, \psi_m = \psi + v_\psi\,, \\ a_{xm} = \dfrac{\bar{q}S}{m}(-C_D\cos\alpha\cos\beta - C_Q\cos\alpha\sin\beta + C_L\sin\alpha) + \dfrac{T}{m} + v_{ax}\,, \\ a_{ym} = \dfrac{\bar{q}S}{m}(-C_D\sin\beta + C_Q\cos\beta) + v_{ay}\,, \\ a_{zm} = \dfrac{\bar{q}S}{m}(-C_D\sin\alpha\cos\beta - C_Q\sin\alpha\sin\beta - C_L\cos\alpha) + v_{az}\,. \end{cases} \tag{2}$$

All the values with a subscript of "m" are observed quantity in above formulas, which are the actual measured value containing measured noise v and denoted as $Z$; the corrected value which minuses the measured noise is equate to the numerical integration result of dynamic differential equations with six degrees of freedom and denoted as $Y$.

According to the observed quantity $Z$ and the dynamic numerical integration result $Y$, the fitness function is designed as:

$$J = (Z - Y)^T Q(z - Y)\,. \tag{3}$$

$Q$ is weight matrix in above formula. The parameters to be identified in aerodynamic model shall be optimized by optimization algorithm to minimize the value of fitness function, and then the identification of aerodynamic parameter will be finished.

## 3. Closed-loop spatial identification based on correlation function estimation

The block matrix of identification framework is filled by the correlation function estimation and null-space projection carried out later to obtain the range of extended observable matrix. This is the basic step of spatial identification method. After that basing on the same projection on time migration set of relevant data, a dynamic estimation of known multivariable bilinear unmanned aerial vehicle system model can be obtained.

### *3.1. Equation of block matrix data estimation*

Construct the block Hankel matrix of correlation function estimation $\hat{R}^{yr}_{\tau_0|\tau_{i-1}}$ and $\hat{R}^{ur}_{\tau_0|\tau_{i-1}}$, including $i$ rows and $j$ columns. The specific definition is as follows:

$$\hat{R}^{yr}_{\tau_0|\tau_{i-1}} = \begin{bmatrix} \hat{R}_{yr}(\tau_0) & \hat{R}_{yr}(\tau_1) & \cdots & \hat{R}_{yr}(\tau_{j-1}) \\ \hat{R}_{yr}(\tau_1) & \hat{R}_{yr}(\tau_2) & \cdots & \hat{R}_{yr}(\tau_j) \\ \vdots & \vdots & \ddots & \vdots \\ \hat{R}_{yr}(\tau_{i-1}) & \hat{R}_{yr}(\tau_i) & \cdots & \hat{R}_{yr}(\tau_{j+i-2}) \end{bmatrix}. \tag{4}$$

$$\hat{R}^{ur}_{\tau_0|\tau_{i-1}} = \begin{bmatrix} \hat{R}_{ur}(\tau_0) & \hat{R}_{ur}(\tau_1) & \cdots & \hat{R}_{ur}(\tau_{j-1}) \\ \hat{R}_{ur}(\tau_1) & \hat{R}_{ur}(\tau_2) & \cdots & \hat{R}_{ur}(\tau_j) \\ \vdots & \vdots & \ddots & \vdots \\ \hat{R}_{ur}(\tau_{i-1}) & \hat{R}_{ur}(\tau_i) & \cdots & \hat{R}_{ur}(\tau_{j+i-2}) \end{bmatrix}. \tag{5}$$

where $\hat{R}^{yr}_{\tau_0|\tau_{i-1}} \in \mathcal{R}^{n_y i \times n_r j}$, $\hat{R}^{ur}_{\tau_0|\tau_{i-1}} \in \mathcal{R}^{n_u i \times n_r j}$. Every element of $\hat{R}^{yr}_{\tau_0|\tau_{i-1}}$ and $\hat{R}^{ur}_{\tau_0|\tau_{i-1}}$ is the data of correlation function, $i$ and $j$ are the subscripts defined by user. According to Formula (4), above matrix meet following condition:

$$\hat{R}^{yr}_{\tau_0|\tau_{i-1}} = \Gamma R^{xr}_{\tau_0} + T_{0|i-1} \hat{R}^{ur}_{\tau_0|\tau_{i-1}}\,. \tag{6}$$

where vector $R^{xr}_{r0}$ is consist of the data of status-cross-correlation functions

$$R^{xr}_{r0} = [R_{xr}(\tau_0) R_{xr}(\tau_1) \cdots R_{xr}(\tau_{j-1})]\,. \tag{7}$$

Then the extended measurement matrix and Toeplitz matrix of lower triangular block respectively are defined as follows:

$$\Gamma = \begin{bmatrix} C_p & C_pA_p & \cdots & C_pA_p^{i-1} \end{bmatrix}^T . \tag{8}$$

$$T_{0|i-1} = \begin{bmatrix} D_p & 0 & \cdots & 0 \\ C_pA_p & D_p & \cdots & 0 \\ \vdots & \vdots & \ddots & \vdots \\ C_pA_p^{i-2}B_p & C_pA_p^{i-3}B_p & \cdots & D_p \end{bmatrix} . \tag{9}$$

By using one step of displacement process, the displacement equation corresponding to Formula (10) can be defined as:

$$\hat{R}^{yr}_{\tau_1|\tau_i} = \Gamma A_p R^{xr}_{\tau_0} + T_{0|i}\hat{R}^{ur}_{\tau_0|\tau_i} \tag{10}$$

where matrix $T_{0|i}$ can be obtained by supplementing the left side with a series of null points. The form is as follows:

$$T_{0|i} = \begin{bmatrix} 0 & D_p & 0 & \cdots & 0 \\ 0 & C_pA_p & D_p & \cdots & 0 \\ \vdots & \vdots & \vdots & \ddots & \vdots \\ 0 & C_pA_p^{i-2}B_p & C_pA_p^{i-3}B_p & \cdots & D_p \end{bmatrix} . \tag{11}$$

Similarly, a row of null point can be added on the bottom of $\hat{R}^{ur}_{\tau_0|\tau_{i-1}}$ to obtain the expression form of $\hat{R}^{ur}_{\tau_0|\tau_i}$ through expansion.

### *3.2. Parameter optimization of spatial identification based on differential evolution*

DE is an algorithm based on population evolution, provided with the characteristics of remembering individual optimal solution or sharing information in population, namely the solution of optimizing the problem by the cooperation and competition between individuals in population [8].

a set of randomly initialized population shall be obtained firstly:

$$X^0 = \left[x_1^0; x_2^0; \cdots; x_{N_p}^0\right] . \tag{12}$$

$N_p$ is the population size, and the individual of $s$th generation can be evolved as follows after a series of specified operations:

$$x_i^s = \left[x_{i,1}^s, x_{i,2}^s, \cdots, x_{i,D}^s\right] . \tag{13}$$

Where $D$ is the dimensionality of the problem optimized.

Add the differential vector obtained by the subtraction of two different random individuals of the parent on 3th individual selected randomly to generate a variant individual. Then carry out a crossover operation between above individuals of the parent and such variant individual in accordance with a certain probability to generate a testing individual. Next make a selection operation between individuals of the parent and such testing individual in accordance with the value of fitness function. The individual with better fitness will be taken as daughter to ensure the evolution is conducted towards optimum [9].

DE/rand/1/bin and DE/best/2/bin: Variation can avoid the local extremum of evolution. There are many methods for it, and 2 basic variation methods are given hereby, DE/rand/1/bin and DE/best/2/bin:

$$x_m = x_{s3}^s + F * (x_{s1}^s - x_{s2}^s) \ , \\ x_m = x_g^s + F * [(x_{s1}^s - x_{s2}^s) \ + (x_{s3}^s - x_{s4}^s) \ ] \ . \tag{14}$$

In Formula (14), $x_{s1}^s, x_{s2}^s, x_{s3}^s, x_{s4}^s$ are the random individuals differing from each other; $x_{gbest}^s$ is the individual with best fitness in current population; $F \in [0, 2]$ is zoom factor,

Crossover strategy: assumed that the testing individual $x_T$ is generated by the crossover operation between $x_i^s$ and $x_m$ in population; in order to ensure the evolution of individuals, $x_T$ shall be contributed by one $x_m$ at least through random selection firstly. Others shall make use of crossover probability factor $CR$, and the crossover operation equation is:

$$x_{Tj} = \begin{cases} x_{mj}, & rand \leq CR \\ x_{ij}, & rand > CR \end{cases} \qquad j = 1, 2, \cdots, D \ . \tag{15}$$

The selection operation adopts the search strategy of "Greedy", in which the individual with highest fitness value will be selected as daughter:

$$x_i^{s+1} = \begin{cases} x_T, & f(x_T) < f(x_i^s) \\ x_i^s, & f(x_T) \geq f(x_i^s) \end{cases} \tag{16}$$

Repeat above operations until the daughter meeting the condition of fitness value is generated, then ended [10–12].

### *3.3. Steps of algorithm*

The specific computational process of closed-loop spatial identification of multivariable bilinear unmanned aerial vehicle proposed in the paper is as shown in Fig. 1. Firstly, obtain the closed-loop prediction on matrix parameter $\Gamma$, $\hat{L}$ and $\hat{G}$ on the base of space projection method. Then obtain the computed values of parameter $\hat{X}$, $A$, $C$ and $\hat{R}$ on the base of matrix manipulation and singular value decomposition process. Finally, solve the system parameter matrix $B$ and $D$ by the algorithm of differential evolution.

In Fig. 1, the solving of $\hat{\Gamma}$ can be figured out according to Formula (28); $\hat{L}$ can be figured out according to Formula (33-34); $\hat{T}$ can be figured out according to Formula

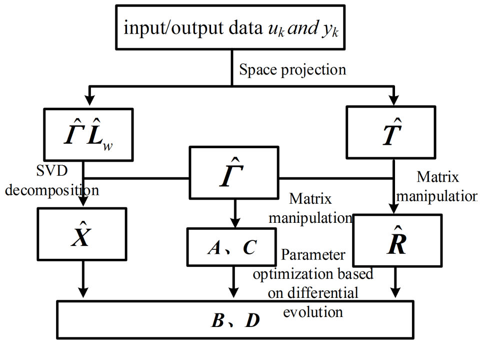


Fig. 1. Process of closed-loop spatial identification

(16); $\hat{X}$ is the state vector matrix of equipment; $A$, $B$, $C$ and $D$ are the state space matrixes, see the part of system dynamics estimation in Section 2.3 for computation process; $\hat{R}$ can be figured out according to Formula (35).

The multivariable bilinear unmanned aerial vehicle used is a low-speed unmanned aerial vehicle with bi-tail-boom layout of a straight wing. The initial condition of simulation is the state of fixed, straight and level flight. The trimming parameters are as follows:

$$\begin{aligned} &V_0 = 35m/S, \alpha_0 = 5.88°, h_0 = 200m \\ &\delta_{e0} = -1.7°, T_0 = 220.87N \end{aligned} \tag{17}$$

As to the longitudinal aerodynamic parameter, only the longitudinal short-period and long-period movement models of unmanned aerial vehicle shall be motivated. For this reason, a combination of "3211" periodic signal with amplitude of $11.46^o$ and a step time interval of 0.3s and the pulse signal with duration of 3s is designed as the simulation input signal of six degree-of-freedom model, and about a half of long-period oscillation time is reserved to obtain more comprehensive characteristics of long-period model of unmanned aerial vehicle. The speed, angle of attack, pitching angle rate and the response curve of pitching angle are shown in Fig. 2. It can be known from the figure that the signal and the combination of long pulse signals successfully motivated obvious short-period and long-period movement models due to the use of "3211".

## 4. Experimental analysis

### *4.1. Experiment settings*

After acquiring the system frequency characteristics and determining the parameter model structure, the system identification has been transformed into a parameter estimation problem: that is, minimize the amplitude and phase error between the expected SISO transfer function $T$ and the corresponding composite frequency

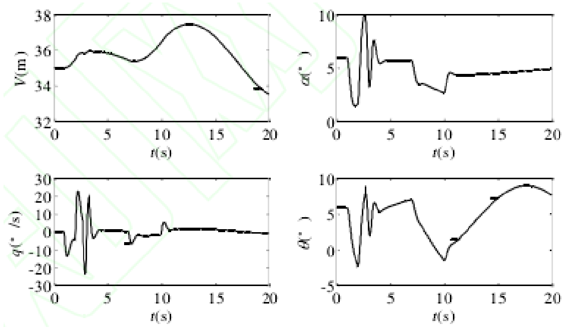


Fig. 2. Longitudinal response curve

response $\hat{T}$ through numerical optimization algorithm. Quadratic cost function:

$$J = \frac{20}{n_\omega} \sum_{\omega_1}^{\omega_{n_w}} W_r \left[ W_g \left( \left| \hat{T}_c \right| - \left| \hat{T} \right| \right)^2 + W_p \left( \angle \hat{T}_c - \angle T \right)^2 \right] . \tag{18}$$

where $\|\|$ is the amplitude at each frequency $\omega$; $\angle$ is the phase of each frequency $\omega$; $n_\omega$ is the number of sampling points of frequency; $\omega_1$ and $\omega_{n_w}$ are the starting frequency and ending frequency value of fitting. The criterion of the cost function:

①When $J \le 100$, it generally reflects the level of accuracy that the flight dynamic model of flight can accept.

②When $J \le 50$, it can be basically expected that it is almost impossible to detect the difference between the fitting results and the flight data.

Therefore, the fitted LOES is within acceptable limits. Fig. 3 is the identification result.

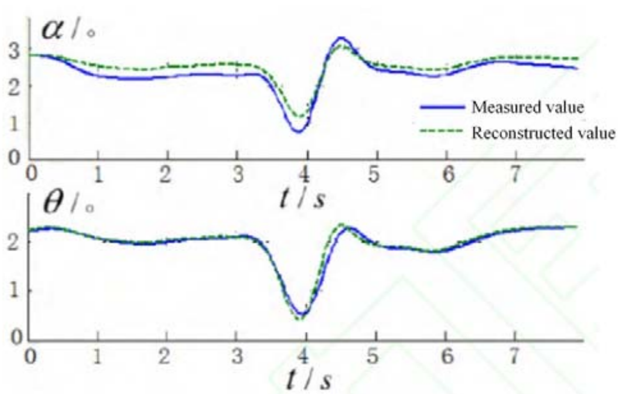


Fig. 3. Identification results

### *4.2. Comparision of identification results*

Three optimization algorithms including GA, PSO and the algorithm in the Paper are respectively used to identify the aerodynamic parameters. The simulation experiment is divided into four groups in accordance with the maximum number of iteration steps, namely, 500, 1000, and 2000, each of which is tested for identification for 50 times. As a preliminary analysis, the test is not added to the observation noise. In order to compare and evaluate the three algorithms as objective as possible, their parameters setting shall stay the same, and use the same fitness function, population size and upper and lower bounds. See Table 1 for identification results.

Table 1. Comparison of identification results

| Parameter | True value | Identified mean value | | |
|---|---|---|---|---|
| | | GA | PSO | Proposed algorithm |
| $C_{D0}$ | 0.06 | 0.0569999 | 0.059909 | 0.06003 |
| $C_{D\alpha}$ | 0.43 | 0.4199999 | 0.430754 | 0.42974 |
| $C_{L0}$ | 0.385 | 0.3749999 | 0.385599 | 0.38474 |
| $C_{L\alpha}$ | 4.78 | 4.7699994 | 4.773452 | 4.78275 |
| $C_{Lq}$ | 10.47 | 10.451354 | 10.35328 | 10.4928 |
| $C_{L\delta_e}$ | 0.201 | 0.2109999 | 0.198585 | 0.20180 |
| $C_{m0}$ | 0.194 | 0.1839999 | 0.194544 | 0.19394 |
| $C_{m\alpha}$ | -2.12 | -2.3200006 | -2.321577 | -2.11936 |
| $C_{mq}$ | -47.6 | -47.51452 | -47.63800 | -47.5840 |
| $C_{m\delta_e}$ | -0.8 | -0.8100001 | -0.810625 | -0.79974 |
| Fitness value | | 121.57 | 289.38 | 84.26 |

Table 1 has compared the average values of the parameters and cost functions on the part of three optimization algorithms successfully identified. From the true value of identification parameters and identification results, all three algorithms have excellent searching ability, PSO algorithm is simple and the mechanism of their overall shared information greatly improves the efficiency of algorithm, but in the later period of the algorithm, because the population position is relatively concentrated, it does not jump out of the local optimal mechanism, making it difficult jump out of local optimum. Compared with GA and PSO algorithm, the algorithm in the Paper has better global searching ability, and the identification value obtained is more accurate.

## 5. Conclusion

A spatial recursive likelihood identification method of multivariable bilinear unmanned aerial vehicle based on differential evolution algorithm is proposed in the paper. It takes dynamic differential equations of rigid body with six degrees of freedom as main governing equation, gives the aerodynamic parameter model of multivariable bilinear unmanned aerial vehicle, and proposes a spatial recursive likelihood identification method based on differential evolution algorithm to achieve the effective identification on model. The effectiveness of algorithm has been verified by the experimental result. The main problem exist in the algorithm proposed in this paper is that the computational complexity shall be further optimized.

## Acknowledgement

Key University Science Research Project o Henan Province:Design of real-time monitoring system for air quality, No.16A510024; The Henan Science and Technology Department Foundation of China under, Grant No.172102210114.

### References

[1] Borra-Serrano I, Peña J M, Torres-Sánchez J, et al.: (2015) *Spatial Quality Evaluation of Resampled Unmanned Aerial Vehicle-Imagery for Weed Mapping*[J]. Sensors, 15(8):19688-19708.

[2] Suk J, Lee Y, Kim S, et al.: (2003) *System identification and stability evaluation of an unmanned aerial vehicle from automated flight tests*[J]. Journal of Mechanical Science and Technology, 17(5):654-667.

[3] Orduyilmaz A: (2006) *Automated image registration and mosaicking for multi-sensor images acquired by a miniature unmanned aerial vehicle platform*[J].

[4] Wang C, He X, Wang X, et al.: (2016) *Distribution characteristics of pesticide application droplets deposition of unmanned aerial vehicle based on testing method of deposition quality balance*[J]. Transactions of the Chinese Society of Agricultural Engineering.

[5] Schouwenaars T, Valenti M J, Feron E, et al.: (1971) *Linear Programming and Language Processing for Human-Unmanned Aerial-Vehicle Team Missions*[J]. Journal of Guidance Control & Dynamics, 29(2):303-313.

[6] Prasanth R K, Boskovic J D, Li S M, et al.: (2001) *Initial study of autonomous trajectory generation for unmanned aerial vehicles*[C]// Decision and Control, 2001. Proceedings of the, IEEE Conference on. IEEE, 2001:640-645 vol.1.

[7] Lelong C C D, Burger P, Jubelin G, et al.: (2008) *Assessment of Unmanned Aerial Vehicles Imagery for Quantitative Monitoring of Wheat Crop in Small Plots*[J]. Sensors, 8(5):3557-3585.

[8] Devernay F, Faugeras O: (2001) *Straight lines have to be straight: automatic calibration and removal of distortion from scenes of structured enviroments*[J]. Machine Vision & Applications, 13(1):14-24.

[9] Taylor L R, Woiwod I P, Perry J N: (1978) *The Density-Dependence of Spatial Behaviour and the Rarity of Randomness*[J]. Journal of Animal Ecology, 47(2):383-406.

[10] Otto G P, Chau T: (1989) *"Region-growing" algorithm for matching of terrain images.*[J]. Image & Vision Computing, 7(2):83-94.

[11] Ghias R, Mittal R, Dong H: (2007) *A sharp interface immersed boundary method for compressible viscous flows*[J]. Journal of Computational Physics, 225(1):528-553.

[12] Paul F, Haeberli W: (2008) *Spatial variability of glacier elevation changes in the Swiss Alps obtained from two digital elevation models*[J]. Geophysical Research Letters, 35(21):189-203.

Received May 7, 2017